Molecular Dynamics Simulations of Sodium Dodecyl Sulfate Micelle in Water: The Behavior of Water

Chrystal D. Bruce,[†] Sanjib Senapati,[‡] Max L. Berkowitz,* Lalith Perera,[§] and Malcolm D. E. Forbes[||]

Department of Chemistry, University of North Carolina at Chapel Hill, CB#3290 Venable and Kenan Labs, Chapel Hill, North Carolina 27514

Received: April 1, 2002; In Final Form: July 22, 2002

Using a 5 ns explicit atom molecular dynamics simulation of a 60 monomer sodium dodecyl sulfate micellar system containing 7579 TIP3P water molecules, the behavior of water in different electrostatic environments was examined. Structural evaluation of the system revealed that penetration of water molecules into the micelle was restricted to the headgroup region, leaving a 12 Å water-free hydrocarbon core. Water molecules near the headgroup exhibit a distortion of the water−water hydrogen bonding network due to headgroup oxygen−water hydrogen bond formation. The dynamic implications of this distortion are manifested in the decay of the dipole autocorrelation function, $\Phi(t)$ and translational diffusion coefficient. We observe that while the translational diffusion coefficient of water molecules in the first solvation shell of the micelle is reduced by less than a half of its value in bulk water, the slow component of the reorientational correlation function is slowed by one or two orders of magnitude.

Introduction

The behavior of water at the molecular level has long been of interest due to its abundance in nature and its unique properties as a solvent.[1−3] In particular, the structure and dynamics of water have been studied in relation to its function in biological systems.[4] Investigations of protein and DNA systems have revealed much about the function of water in the stability of these macromolecules[5] and its role in moving ions across ion channels.[6−8] Through a combination of experimental and computational techniques, properties such as hydrogen bonding, diffusion, and reorientation in response to stimuli can be probed.[9] With greater computing power becoming available, increasingly complex systems can now be examined. Thus, for example, the structural and dynamical properties of micellar solutions can be studied using molecular dynamics simulations.[10−23] From these simulations we can also learn about the molecular level structure and dynamics of water in charged environments and its interaction with such charged assemblies.

The formation of a micelle is dependent on the presence of water in large quantities relative to the surfactant. The surfactant aggregates with other surfactant molecules to minimize the energetically unfavorable interaction of its hydrophobic tail with water. In this work, the water molecules have been explicitly simulated as opposed to using an electrostatic continuum description for the water. Since individual water molecules can control the outcome of many fundamental processes, water should be studied both macroscopically and as individual molecules composing the solvent.

The common ionic surfactant sodium dodecyl sulfate (SDS) is shown in Scheme 1 with the hydrophobic and hydrophilic regions labeled. Hydrogens are not shown for clarity. Micelles formed from SDS have been studied previously using molecular dynamics[17,19] and other computer simulation techniques, but the time scale and system size in all of these previous studies were small compared to our recent more extensive calculations.[10] Our longer simulation (5 ns) has shown that the sodium counterions require a significant amount of equilibration time. Another benefit of using a larger system is that better statistics becomes available for certain physical properties of water, such as the diffusion coefficient in different regions of the system. Of the micellar characteristics evaluated in our previous work (we will refer to this as Paper I), none had significant deviation over time except for the required equilibration time for the sodium counterion distribution. This was accounted for in the analysis by discarding the first nanosecond of the production run. The same procedure is followed here. All micellar structural quantities were stable throughout the simulation.

SCHEME 1

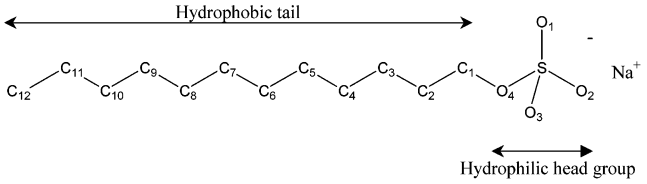

Paper I reported a detailed analysis of the structural and dynamical properties of the surfactant molecules and the Na^+ counterions. The results implied that a large amount of surface roughness exists in the system. Hydrocarbon-to-water contact was evaluated on the basis of accessible surface area calculations. Evaluation of the micelle shape revealed that the micelle is not completely spherical, but has ellipsoidal components. In addition, the surfactant monomers were not all perfectly arranged around the center of the micelle, but, instead, oriented themselves in a variety of directions toward and away from the

* Corresponding author. E-mail: maxb@unc.edu.
[†] E-mail: cbruce@email.unc.edu.
[‡] E-mail: sanjib@email.unc.edu.
[§] E-mail: lalith_perera@unc.edu.
[||] E-mail: mdef@unc.edu.

10.1021/jp025872x CCC: $22.00
Published on Web 09/28/2002

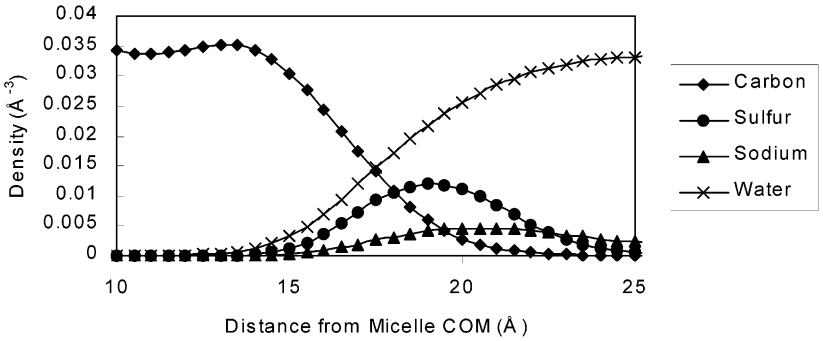

Figure 1. Density of selected atoms at the interfacial region between the micelle and the aqueous phase.

hydrocarbon core while still generally associating with the other tails.

It was also observed that the sodium ions formed contact-ion pairs with the micelle headgroups rather than completely dissociating. Fifty percent of the counterions were in either the first or second shell while the remainder were in the bulk. The diffusion coefficients for the ions in these different regions were all less than D_{Na^+} found for a system consisting of spatially separated Na^+ and Cl^- in water. In addition, the diffusion coefficients for the ions followed the trend $D_{3rd\ shell} > D_{2nd\ shell} > D_{1st\ shell}$. Below, this pattern for the sodium ions in different shells will be compared to the pattern for water molecules in different regions of the system.

To complete our study of the structural and dynamical properties of the SDS micellar solution, an examination of the properties of water in this system was done. In previous computational studies of SDS by other researchers only structural analyses through the relevant radial distribution functions were performed. No dynamic studies of the water behavior were carried out.[17,19] Water coordination distributions were not analyzed and neither was the hydrogen bonding network or the diffusion coefficients. Comparison of these properties was reported in one series of papers on sodium octanoate micelles, but this surfactant has a very different headgroup and will clearly exert a different influence on the water behavior than SDS.[14−16] Studies of octyl glucoside micelles performed by Bogusz et al.[21,22] examined the structure of the waters interacting with the micelle, but did not report any results on the bulk behavior or on any of the water dynamics. The work of Tieleman et al.[18] on dodecylphosphocholine considered only the physical properties of the micelle/water interface. Clearly there is a need for a detailed analysis of the behavior of water in different regions of SDS micelles, and we will use our MD run for this purpose. Below we present results of our analysis with particular attention paid to structural issues such as electrostatic environment and penetration of water into the micelle core, and to dynamic issues such as the diffusion coefficient.

Method

The simulation was carried out as described in detail in Paper I.[10] Briefly, the method is summarized as follows: The parm98 force field within AMBER 6[24] was used to perform a 5 ns NVT molecular dynamics simulation on a SDS micelle consisting of 60 surfactant monomers, 60 Na^+ counterions, and 7579 TIP3P[25] water molecules. Thermalization and equilibration were carried out including a 40 ps NPT simulation, which brought the density to 1.0051 g/mL and a box size of 65.042 Å × 61.762 Å × 63.348 Å. A 2 fs time step was used for the production run with SHAKE for all hydrogen-containing bonds and the Berendsen temperature coupling method[26] to keep the temperature at 300 K. For comparison, a simulation consisting of 510 TIP3P water molecules was performed at 300 K in a periodic box of dimension 24.837 Å × 24.837 Å × 24.837 Å. A 400 ps NVT production run was carried out after a short (100 step) minimization, an NPT simulation for density equilibration, and thermalization.

Further explanation of the methods used to extract physical properties of the system are given in the relevant sections below. As mentioned previously, one of the most distinct differences between this work and all previous studies of ionic surfactant systems is the length of the simulation: 5 ns. During this simulation the sodium counterions required a full nanosecond to reach an equilibrated distribution. As a result, complete analysis of the system was performed only on the last 4 ns of the simulation.

Results and Discussion

A. Water Structure. *1. Interfacial Region and Water Penetration.* The density distribution of selected atoms in the system provides information about its composition. A radial density plot (Figure 1) was constructed by calculating the distance of selected atoms from the micelle center of mass (COM) every 1 ps and counting the number of atoms in 0.1 Å wide shells around the micelle COM. Examination of Figure 1 shows that the interior of the micelle is water free. There is a 10 Å portion (from $R = 12$ Å to $R = 22$ Å) where the hydrocarbon and water are in contact. This value is comparable to those obtained in studies of dilauroylphosphatidylethanolamine (DLPE) and dipalmitoylphosphatidylcholine (DPPC) membranes.[27] The length of the interface, defined as the distance between the point where the water reaches 10% of its bulk density and the point where the hydrocarbon diminishes to 10% of its bulk density, is 4.5 Å. This is in agreement with results of MacKerrell.[17] The 12 Å water-free hydrocarbon core also agrees with MacKerrell, but in that work water molecules within 12 Å of the micelle COM were removed as part of the setup prior to the production run. No water molecules were deleted in this manner in our simulations because there were no water molecules within 12 Å of the micelle COM after the thermalization process of the system preparation.

Investigation of the interface between the bulk water and the micelle interior reveals a region where the water molecules interact with both the hydrophilic headgroup and the hydrophobic tail of the micelle. Because there are not enough headgroups to completely cover the micelle surface, there is some water-to-hydrocarbon contact. The accessible surface area analysis presented in Paper I revealed that 70% of the micelle-to-water contact is through the headgroup. Therefore, it is the oxygen atoms of the headgroup that provide the primary means

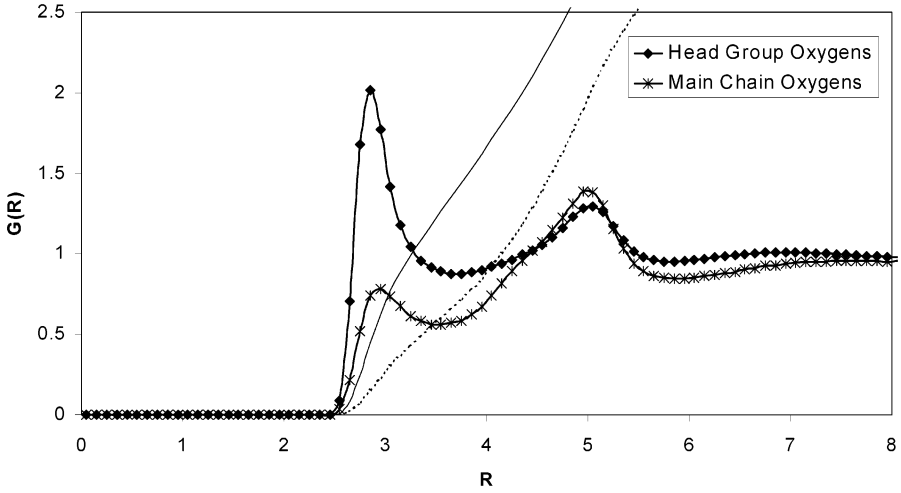

Figure 2. Water oxygens-to-micelle oxygens radial distribution function. Headgroup oxygens = O_{1-3}. Main chain oxygen = O_4. Thin solid line shows the coordination number of the headgroup oxygen, while dashed solid line is for the main chain oxygen. The number of water molecules in the first coordination shell is 0.6 for O_4 and 1.3 for O_1, O_2, and O_3.

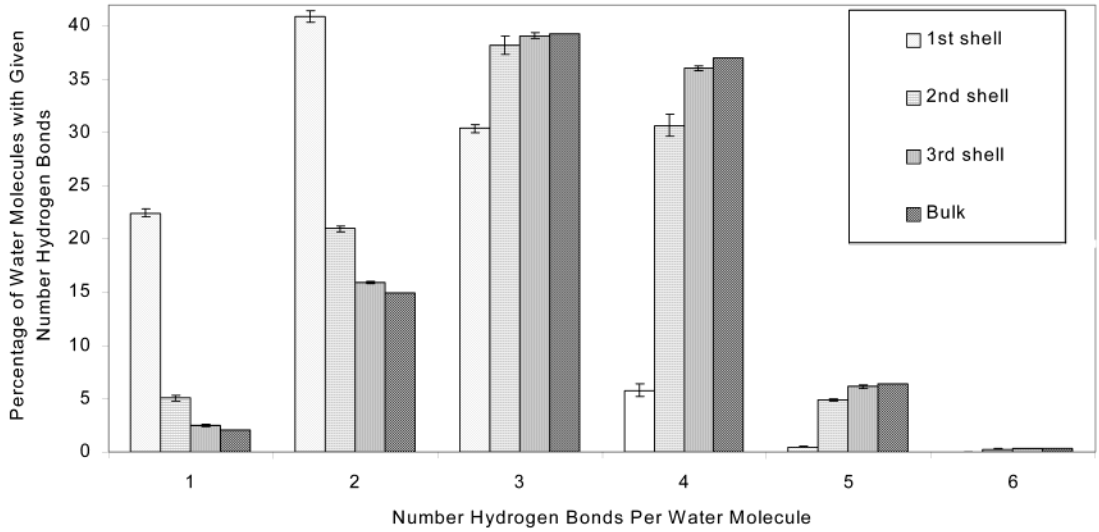

Figure 3. Water−water hydrogen bonding by micellar region. The *y*-axis represents the percentage of water molecules with a given number of hydrogen bonds.

of micelle-to-water electrostatic interactions. Complete characterization of the interface between the micelle and the water is important as it can aid in the understanding of how other hydrophilic species such as cells and membranes interact with their aqueous environments.

2. Hydrogen Bonding Network. To analyze the water−headgroup interaction, relevant radial distribution functions (RDFs) were calculated over the last 4 ns of the simulation at 2 ps intervals. These functions were then averaged and normalized. Figure 2 shows the RDFs for both O_4 and O_{1-3} to water oxygen (see Scheme 1 for explanation of the numbering system). At a course glance, it may seem odd that the peaks of the RDF are coincident, but further investigation reveals that surfactant monomers can extend into the water enough that O_4 is at the same distance from a water molecule as O_{1-3}. The difference in the magnitudes of the peaks more clearly expresses the difference in the relative position along the chain of O_4 compared to O_{1-3}. It should be noted that the RDFs are normalized so that the difference in magnitude is not simply due to the fact that there are three terminal oxygens atoms on the headgroup and only one main chain oxygen atom.

The presence of the surfactant headgroup causes many distortions in the bulk behavior of water near the micelle. One of the most distinctive features of bulk water is its hydrogen bonding network. Disruption of the network in different regions of the system was quantified using the energetic definition of a hydrogen bond: when the pair energy of any two water molecules is less than −10 kJ/mol, the waters are considered to be hydrogen bonded. Figure 3 shows the results of our analysis for water-to-water hydrogen bonding distribution. The analysis was performed for different shells of water. Based on the micelle oxygen-to-water oxygen radial distribution function (Figure 2), each shell was defined as follows:

$$\text{First Shell of Water:} \quad R_{O_w-O_{mic}} < 3.5\ \text{Å} \tag{1}$$

$$\text{Second Shell of Water:} \quad 3.5\ \text{Å} < R_{O_w-O_{mic}} < 6.0\ \text{Å} \tag{2}$$

$$\text{Third Shell of Water:} \quad R_{O_w-O_{mic}} > 6.0\ \text{Å} \tag{3}$$

Comparisons were made with a bulk water simulation performed on 510 TIP3P water molecules. Third shell water molecules exhibit a nearly identical distribution of hydrogen bonds as that of bulk water: most of the water molecules have 3 hydrogen bonds followed by 4 and then 2.[25,28] (The relative proportions

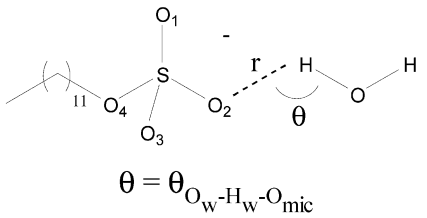

Figure 4. Water-to-surfactant hydrogen bonding. A water molecule is considered hydrogen bonded to the micelle if $R_{O_w-O_{mic}} < 3.25$ Å and $\theta_{O_w-H_w-O_{mic}} > 140°$.

for bulk water depicted in Figure 3 differ slightly from that of Jorgensen et al. since they use an energetic definition of a hydrogen bond of −2.25 kcal/mol (or −9.414 kJ/mol). When −9.414 kJ/mol was used as the energetic criterion, the Jorgensen distribution was reproduced. The differences, though, are extremely small, and thus a cutoff of −10.0 kJ/mol was used for all water-to-water hydrogen bond calculations).

The hydrogen bond distribution for the second shell of water is different compared to that of bulk water. Thus, for example, we observe a decrease in the relative ratio of 4 and 2 hydrogen bonds from 2.4:1 in bulk to 1.5:1 in the second shell. For water molecules in the first shell of the micelle, the presence of the headgroups (as well as their charge) causes a much greater distortion in this distribution. Here the majority of the water molecules have only 2 water-to-water hydrogen bonds and a significant decrease is observed in the number of water molecules with 4 water-to-water hydrogen bonds. It is interesting to note that the percentage of water molecules having n hydrogen bonds in the first shell is comparable to the percentage of water molecules having $n + 1$ hydrogen bonds in either of the other two shells or in the bulk water simulation. This can be explained by considering that in the first shell of the micelle, micelle headgroup atoms may replace the position normally filled by another water molecule with a hydrogen bond to the micelle through the headgroup oxygen atoms. This phenomenon was investigated by stipulating that a micelle-to-water hydrogen bond exists when the distance between the water oxygen and the micelle oxygen is less than 3.25 Å and the angle θ formed by the micelle oxygen, one of the water hydrogens, and the water oxygen was greater than 140°. (See Figure 4.)

Evaluation of the water-to-micelle oxygen hydrogen bonding reveals that 60% of the water molecules in the first shell of the micelle have one micelle-to-water hydrogen bond and 33% have zero. (See Figure 5.) Combining this information with the water-to-water hydrogen bonding for first shell water molecules (distribution shown in Figure 3) results in a total hydrogen bonding distribution for first shell water molecules that more closely resembles that of bulk water (See Figure 6), although the distribution shifts toward a fewer number of hydrogen bonds per water molecule. As will be discussed below, this shift has a significant impact on the mobility of the water molecules in the first shell. It must be noted that the relative distributions of hydrogen bonds shown in Figure 5 depend somewhat on the choice of hydrogen bond definition although for variations of $\theta \pm 20°$, the most noticeable difference was the exact number of hydrogen bonds, not the relative ratios.

Continuing with this definition of a micelle-to-water hydrogen bond, the number of water molecules that are hydrogen bonded

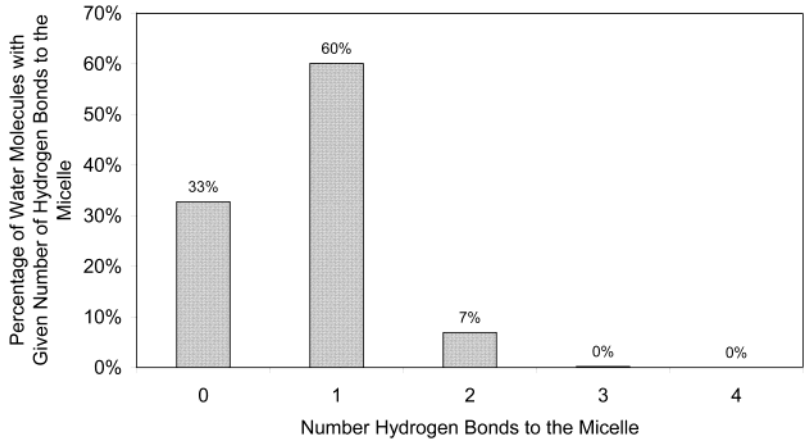

Figure 5. Water-to-micelle hydrogen bonding distribution.

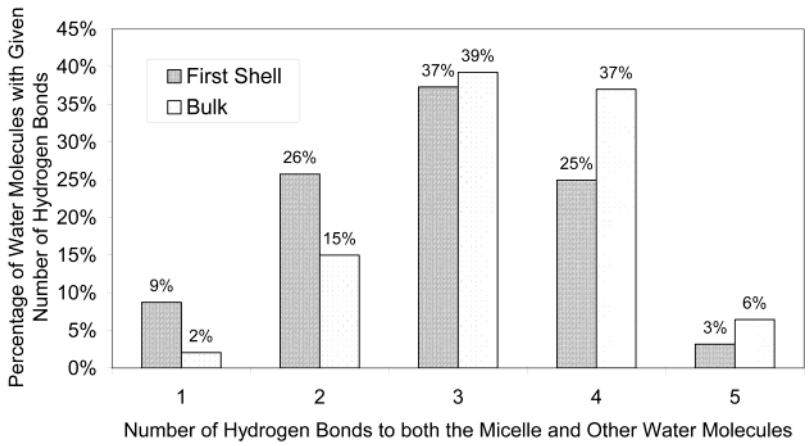

Figure 6. Average number of hydrogen bonds per water molecule in the first shell including water−water hydrogen bonding and water−micelle hydrogen bonding.

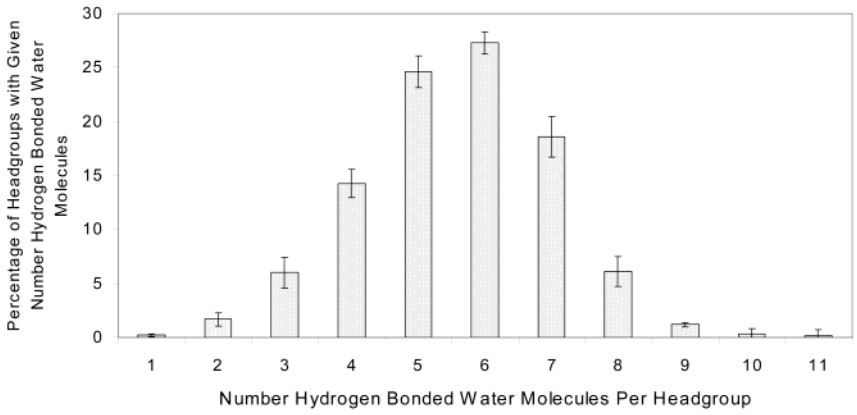

Figure 7. Water coordination around micelle headgroup. Water-to-micelle hydrogen bond defined in Figure 5.

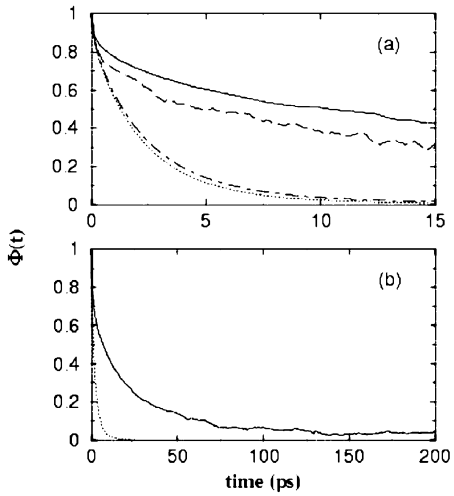

Figure 8. (a) The single dipole autocorrelation function as a function of time for those water molecules that remain in respective shells continuously for 20 ps; the solid line is for water molecules in the first shell, the long dashed line is for water in the second shell, and the dot−dashed line is for water in the third shell. For comparison, the decay of bulk water is also included (dotted line). (b). Dipolar autocorrelation function for those water molecules which stay at a distance less than 6 Å from the micellar surface continuously for 250 ps (solid line). The dotted line is for bulk water.

to an individual headgroup (or coordination number) was also examined. The resulting distribution is shown in Figure 7. It was found that 70% of the monomer headgroups have from 5 to 7 water molecules hydrogen bonded to them. Detailed analysis of the hydrogen bonding network of water in the different regions of the micelle and of water-to-micelle hydrogen bonding are crucial in understanding the structure and dynamics of water in confined environments, and it is to the issue of dynamics that we now turn.

B. Water Dynamics. *1. Dipole Autocorrelation Functions.* The single dipole autocorrelation function, $\Phi(t)$, provides information on the reorientation of the solvent (through motion of its dipole) as a result of interaction with other solvent dipoles or solute molecules over time. $\Phi(t)$ is defined as[29]

$$\Phi(t) = \frac{\langle \mu(t) \cdot \mu(0) \rangle}{\mu^2} \tag{4}$$

where $\mu(t)$ is the dipole of a given water molecule at a time t and $\mu(0)$ is the dipole of the same water molecule at time zero. Figure 8a shows $\Phi(t)$ as a function of time for water molecules in each of the three shells of the micelle as well as that for bulk water. Each curve (except the curve for bulk water) was obtained from 20 ps trajectories during which water molecules were in their corresponding shells and did not cross the boundaries of these shells. As we can see, while over the first 100 fs the dipole autocorrelation function for water molecules in the first shell displays an initial decay that is the same as for bulk water molecules, over the longer time scale the decay is much slower compared to the one observed for bulk water molecules. The behavior of the autocorrelation function of the water molecules in the second shell is similar to the one displayed for the first shell, although the slow component decay is somewhat faster. Finally, we observe that the decay of the correlation function for those water molecules that are in the third shell is the same as the decay for bulk water molecules. To find out the behavior of the orientational correlation function over longer time we need to take into account that water molecules cross the boundaries of the shells over longer times. Thus to extend our calculation of the correlation function to a 200 ps time interval we divide all water molecules into two groups: the first group contains all the water molecules that are influenced by the micelle, i.e., water molecules that stay at a distance less than 6 Å from the micelle during the time interval of 250 ps, the second group contains all other water molecules. Figure 8b shows the plot of the dipole autocorrelation function for water molecules that are influenced by the surface of the micelle and compare this plot with the one for bulk water. From both Figures 8a and 8b we conclude that the slow component of the reorientational correlation function decays much slower (by one or 2 orders of magnitude) compared to bulk water.

2. Diffusion Coefficients. It has already been confirmed that the micelle significantly distorts the structural properties of water molecules next to the micellar surface. We also observed that the rotational dynamics of a water molecule next to the surface is disturbed. The translational dynamics of the water can be appropriately examined by comparing the relative diffusion coefficients in different parts of the system. Using Einstein's relation connecting mean square displacement with the diffusion coefficient:

$$D = \lim_{t \to \infty} \frac{\langle |r(t) - r(0)|^2 \rangle}{6t} \tag{5}$$

and the water-to-micelle oxygen RDF (Figure 2) to define shells of water that surround the micelle, we found that the relative ratio of diffusion coefficients for water molecules in the three regions is roughly 0.6:0.8:1 with a value for $D_{\text{3rd shell}}$ of 5.4×10^{-5} cm^2/s. This value is comparable to that found previously for the TIP3P water model.[30,31] D_{bulk} was found to be 5.3×10^{-5} cm^2/s. Equations 1−3 give the definitions for water shells

used in this analysis. Again, as for the calculations of dipole autocorrelation functions, the 20 ps trajectories were used for all three shells to determine the diffusion coefficient.

Conclusions

It is clear from both structural and dynamical analyses that the water molecules in the first shell of the micelle experience a different environment than those in the rest of the system because of interaction with the micelle headgroup. We observed that the pattern of hydrogen bonding for water molecules near the surface of the micelle is changed. Since the deviations in hydrogen bonding network produce changes in diffusion coefficients,[33] we expect that diffusion coefficients for restricted water next to the micelle will differ from the one observed for bulk water. In recent work on the kinetic behavior of the hydrogen bonding network, the relationship between diffusion and hydrogen bonding is described as a cooperative effort between adjacent water molecules.[34,35] For a hydrogen bond to break, there must be another water molecule available to form a new hydrogen bond. Without the impetus to hydrogen bond to a different water molecule, it is unlikely that the first hydrogen bond will be broken. In our work, the disruption of the hydrogen bonding network by the micelle results in fewer adjacent water molecules available for hydrogen bond formation, which is evidenced by a decrease in the self-diffusion coefficient. The smaller differences in the hydrogen bonding network in the second shell and bulk water molecules also provide the clues needed to explain the difference in diffusion coefficient between the second shell and bulk.

While the translational diffusion of water molecules in the first solvation shell of the micelle is reduced by less than a half of its value in bulk water, the slow component of the reorientational correlation function is slowed by one or two orders of magnitude. This reduction in the mobility of water molecules next to the micelle is perhaps due to the locking of water molecules into certain configurations, again due to strong hydrogen bonding. Water molecules in the second shell around the micelle also display substantial deviations in their structural and dynamical properties compared to bulk water properties. Water molecules beyond the second shell display properties very similar to bulk properties, demonstrating that in our system there is a limited range of order imposed by the presence of the micelle and the sodium counterions. This is consistent with results presented by Faeder and Ladanyi using MD to study the interior of a model aqueous reverse micelle.[32] They find that the distortion of water properties such as hydrogen bonding occurs only within a few molecular diameters of the interface and the bulk water properties are again observed a larger distances from the interface. Our results on the substantial slowing down of the reorientational motion of water molecules that are influenced by the presence of the micelle are consistent with the observation made by Bagchi and his collaborators.[9,36,37] Bagchi and collaborators pointed out[36] that confined water responds to solute change in a bimodal way, with one fast bulk water-like subpicosecond component and a slow component on a time scale of hundreds or thousands of picoseconds. Very recently Balasubramanian et al.[37] studied water dynamics at the surface of cesium pentadecafluorooctanoate and observed that the reorientational motion of water near the micelle is restricted, and as a result it exhibits a slow component which is slower than its bulk value by at least two orders of magnitude. Although the value by which the slow component is slowed depends on the details of the system and even the details of the analysis performed, the qualitative conclusion obtained from experiments[37] and simulations is that constrained water exhibits slow dynamics. This has substantial implications for kinetics of reactions occurring in the presence of this type of water.

Acknowledgment. The authors thank the North Carolina Supercomputing Center for CPU time, the UNC-CH computing center for use of its facilities, and the National Science Foundation (Grant CHE-9820791). C.D.B. also thanks NSF's graduate fellowship program for financial support. This work was also partially supported by the STC Program of the National Science Foundation under Agreement CHE-9876674.

References and Notes

(1) Eisenberg, D. S.; Kauzmann, W. *The Structure and Properties of Water*; Clarendon Press: Oxford, 1969; p 296.
(2) Stillinger, F. H. *Science* **1980**, *209*, 451.
(3) *Water, a Comprehensive Treatise*; Franks, F., Ed.; Plenum Press: New York, 1972−1982.
(4) Finney, J. L. *Faraday Discuss.* **1996**, *103*, 1−18.
(5) Gorokhov, A.; Perera, L.; Darden, T. A.; Negishi, M.; Pedersen, L. C.; Pedersen, L. G. *Biophys. J.* **2000**, *79*, 2909.
(6) Sansom, M. S.; Kerr, I. D.; Breed, J.; Sankararamakrishnan, R. *Biophys. J.* **1996**, *70*, 693.
(7) Tieleman, D. P.; Berendsen, H. J. C.; Sansom, M. S. *Biophys. J.* **1999**, *76*.
(8) Roux, B.; Nina, M.; Pomes, R.; Smith, J. C. *Biophys. J.* **1996**, *71*, 670.
(9) Nandi, N.; Bhattacharyya, K.; Bagchi, B. *Chem. Rev.* **2000**, *100*, 2013−2045.
(10) Bruce, C. D.; Berkowitz, M. L.; Perera, L.; Forbes, M. D. E. *J. Phys. Chem. B* **2002**, *106*, 3788.
(11) Watanabe, K.; Ferrario, M.; Klein, M. *J. Phys. Chem.* **1988**, *92*, 819.
(12) Jonsson, B.; Edholm, O.; Teleman, O. *J. Chem. Phys.* **1986**, *85*, 2259.
(13) Kuhn, H.; Breitzke, B.; Rehage, H. *Colloid Polym. Sci.* **1998**, *276*, 824.
(14) Kuhn, H.; Rehage, H. *Ber. Bunsen-Ges.* **1997**, *101*, 1493.
(15) Kuhn, H.; Rehage, H. *Ber. Bunsen-Ges.* **1997**, *101*, 1485.
(16) Kuhn, H.; Rehage, H. *Prog. Colloid Polym. Sci.* **1998**, *111*, 158.
(17) MacKerell, A. *J. Phys. Chem.* **1995**, *99*, 1846.
(18) Tieleman, D. P.; van der Spoel, D.; Berendsen, H. J. C. *J. Phys. Chem. B* **2000**, *104*, 6380.
(19) Shelley, J.; Watanabe, K.; Klein, M. *Int. J. Quantum Chem: Quantum Biol. Sym.* **1990**, *17*, 103−117.
(20) Wendoloski, J. J.; Kimatian, S. J.; Schutt, C. E.; Salemme, F. R. *Science* **1989**, *243*, 636.
(21) Bogusz, S.; Venable, R. M.; Pastor, R. W. *J. Phys. Chem. B* **2000**, *104*, 5462.
(22) Bogusz, S.; Venable, R. M.; Pastor, R. W. *J. Phys. Chem. B* **2001**, *105*, 8312.
(23) Marrink, S. J.; Tieleman, D. P.; Mark, A. E. *J. Phys. Chem. B* **2000**, *104*, 12165.
(24) Case, D. A.; Pearlman, D. A.; Caldwell, J. W.; Cheatham, T. E., III; Ross, W. S.; Simmerling, C. L.; Darden, T. A.; Merz, K. M.; Stanton, R. V.; Cheng, A. L.; Vincent, J. J.; Crowley, M.; Tsui, V.; Radmer, R. J.; Duan, Y.; Pitera, J.; Massova, I.; Seibel, G. L.; Singh, U. C.; Weiner, P. K.; Kollman, P. A. *AMBER 6, University of California, San Francisco*, 1999.
(25) Jorgensen, W. L.; Chandrasekhar, J.; Madura, J. D.; Impey, R. W.; Klein, M. L. *J. Chem. Phys.* **1983**, *79*, 926.
(26) Berendsen, H. J. C.; Postma, J. P. M.; Van Gunsteren, W. F.; DiNola, A.; Haak, J. R. *J. Chem. Phys.* **1984**, *81*, 3684.
(27) Perera, L.; Essmann, U.; Berkowitz, M. *Langmuir* **1996**, *12*, 2625−2629.
(28) Vaisman, I. I.; Perera, L.; Berkowitz, M. L. *J. Chem. Phys.* **1993**, *98*, 9859.
(29) Perera, L.; Berkowitz, M. L. *J. Chem. Phys.* **1992**, *96*.
(30) Mark, P.; Nilsson, L. *J. Phys. Chem. A* **2001**, *105*, 9954.
(31) van der Spoel, D.; van Maaren, P.; Berendsen, H. J. C. *J. Chem. Phys.* **1998**, *108*, 10220.
(32) Faeder, J.; Ladanyi, B. M. *J. Phys. Chem. B* **2000**, *104*, 1033.
(33) Starr, F. W.; Neilsen, J. K.; Stanley, H. E. *Phys. Rev. E* **2000**, *62*, 579.
(34) Luzar, A.; Chandler, D. *Nature* **1996**, *379*, 55.
(35) Xu, H.; Berne, B. J. *J. Phys. Chem. B* **2001**, *105*, 11929.
(36) Bhattacharyya, K.; Bagchi, B. *J. Phys. Chem. B* **2000,** 104, 10603.
(37) Balasubramanian, S.; Pal, S.; Bagchi, B. *Curr. Sci.* **2002**, 82, 845.